water

MDPI

Article

The Impacts of Different Salinities on the CW-MFC System for Treating Concentrated Brine

Li Wang [1,*,†], Xuwei Han [1,†], Yu Zhang [2,†], Lin Wang [3] and Jin Wang [1]

1 School of Energy Science and Engineering, Harbin Institute of Technology, Harbin 150001, China; hanxuwei2000@163.com (X.H.); wangjin000704@163.com (J.W.)
2 College of Engineering Management, Ocean University, Qingdao 266100, China; wfeebzhangyu@163.com
3 School of Environmental Science and Engineering, Ocean University, Qingdao 266100, China; lwangouc@126.com
* Correspondence: liwanghit@126.com; Tel.: +86-13304808087
† These authors contributed equally to this work.

Abstract: This paper aims to comprehensively explore the performance and influencing factors of the constructed wetland–microbial fuel cell (CW-MFC) system when treating brine with different concentrations. The main objective is to determine how different salinity levels affect the operation and treatment efficiency of the CW-MFC system. The research results show that Bruguiera gymnorrhiza exhibits strong salt tolerance and can be used as a wetland plant for the CW-MFC system. The closed-circuit CW-MFC system with planted plants has the best performance, with a chemical oxygen demand (COD) removal rate of 84.8%, a total nitrogen (TN) removal rate of 68.12%, and a chloride ion (Cl^-) removal rate of 29.96%. The maximum power density is 64.79% higher than that of the system without planted plants. The power generation performance of the system first increases and then decreases with the increase in salinity, while the internal resistance keeps decreasing. When the salinity is 2%, the power generation effect is the best, with an average output voltage of 617.3 ± 25.7 mV and a power density of 45.83 mW/m^2. The removal rates of COD and TN are inhibited with the increase in salinity, while the removal rate of total phosphorus (TP) is not significantly affected. The microbial community grows well under salt stress, but its structure is different. When the salinity is 1%, the optimal distance between electrodes is 10 cm. Considering the pollutant removal performance, the optimal hydraulic retention time is 3 days, and considering the power generation performance, the optimal hydraulic retention time is 2 days. This research provides important value for improving the performance of the CW-MFC system in treating brine.

Keywords: constructed wetland–microbial fuel cell; seawater desalination brine; pollutant removal; biological power generation

Academic Editor: Vasileios Bartzis

Received: 25 November 2024
Revised: 2 January 2025
Accepted: 15 January 2025
Published: 16 January 2025

Citation: Wang, L.; Han, X.; Zhang, Y.; Wang, L.; Wang, J. The Impacts of Different Salinities on the CW-MFC System for Treating Concentrated Brine. *Water* **2025**, *17*, 247. https://doi.org/10.3390/w17020247

1. Introduction

With the increasingly severe problem of water shortage, seawater desalination, as an important open-source and increment technology of water resources, has received extensive attention [1,2]. Among them, reverse osmosis seawater desalination (SWRO) has been widely used around the world due to its numerous advantages [3]. China's reverse osmosis seawater desalination technology has also achieved great development, and the relevant project scale has been continuously expanding. However, a large amount of concentrated brine will inevitably be produced during the seawater desalination process. Factors such as its salinity, temperature, and pollutants contained therein pose many hazards to the marine ecological environment, such as affecting the growth and reproduction of marine organisms and leading to the eutrophication of water bodies. Therefore, the treatment of concentrated brine has become a key issue that urgently needs to be resolved [4]. Currently, common concentrated brine treatment technologies after seawater desalination are divided into two types: environmentally friendly and traditional, but each has certain limitations. For example, salt-making and membrane separation technologies have high costs and are prone to clogging, and traditional methods such as discharge and deep-well injection have a great impact on the environment or are costly [5,6]. Therefore, it is urgent to seek better treatment technologies.

Microbial fuel cells can recycle wastewater resources and achieve energy recovery [7]. There have already been studies on its application in the field of seawater desalination [8]. Constructed wetland (CW) technology has the advantages of low operating cost and being eco-friendly, and it plays an important role in the treatment of various types of wastewater [9,10]. The MFC device consists of an anode (anaerobic) region and a cathode (aerobic) region, which is highly compatible with the structure and function of the vertical up-flow CW system [11]. The microbial community composition and their relative abundance in CW-MFC have shown a drift from conventional CW with 4.5-fold enhanced COD removal kinetics [12]. Abou-elela, S. I [13] compared the treatment of municipal sewage by horizontal flow and vertical flow constructed wetlands and found that the vertical flow constructed wetlands were more efficient in terms of chemical oxygen demand (COD), biochemical oxygen demand (BOD), and nitrification. Thalla, A.K [14] discovered that the overall removal rate of the vertical flow constructed wetlands was 7.14% higher than that of the horizontal subsurface flow constructed wetlands. Pandey, M. K [15] also reached the same conclusion. Doherty, L [16] conducted a comprehensive review on the systems with different structures of the integrated constructed wetland–microbial fuel cell system, rigorously compared the performance of systems with different structures, and concluded that the vertical flow was more advantageous in terms of oxygen transfer and microorganism distribution, having a more positive effect on power generation efficiency. The vertical up-flow CW-MFC system can make the sewage first pass through the anaerobic anode region and then flow upward with the water to the aerobic cathode region, facilitating the directional transfer of ions [17]. It does not require a proton exchange membrane and has the advantages of a small footprint, easy operation, and rapid removal of pollutants, providing new possibilities for the treatment of concentrated brine from seawater desalination [18]. However, when treating concentrated brine from seawater desalination, its system structure is affected by factors such as plants, microorganisms, electrodes, and substrate materials [19–23], and its operating parameters are restricted by factors such as salinity and hydraulic retention time [24–26]. Although existing studies have recognized the potential of the CW-MFC system in treating concentrated brine from seawater desalination, there has been no exploration of different salinity gradients, nor in-depth research on the influences of plants, microorganisms, electrodes, and substrates within the system, lacking comprehensive investigations of multiple factors.

To sum up, this study constructed an up-flow constructed wetland–microbial fuel cell (CW-MFC) device, and explored the roles of plants, current, microorganisms, and fillers in the system, as well as the treatment effect and power generation performance of concentrated brine under different operating parameters. The influence of different salinities of concentrated brine from seawater desalination on the system efficiency was revealed, and the change of system performance with the salinity gradient was investigated, enabling it to be further extended to a wide range of salinity conditions, providing theoretical support and prediction directions for practical engineering applications. Meanwhile, the CW-MFC system can directly convert chemical energy into electrical energy, realizing the resource utilization of pollutants, with the advantages of sustainability and no secondary pollution.

It has promoted the cross-integration of multiple disciplines and facilitated technological innovation and progress in fields such as microbiology, electrochemistry, and materials. This study has shown great potential and broad application prospects in addressing global energy and environmental challenges.

2. Methods

2.1. Experimental Wastewater

The influent water for the experiment was close to the actual concentrated brine from seawater desalination. Referring to the artificial seawater formulation proposed by Dana R. Kester et al. [27] and consulting relevant literature [28], for instance, to prepare 1% concentrated brine, it was stipulated that 1 g of NaCl was contained in every 100 g of the concentrated brine based on the influent volume. The composition of the artificially simulated concentrated brine from seawater desalination, excluding NaCl, is presented in Table 1. Since the salinity of concentrated brine from seawater desalination usually exceeds 3% and thus belongs to high-salinity wastewater, considering the tolerance of wetland plants and the reproduction and metabolism of microorganisms within the system, this study set relatively low salinity gradients (1%, 2%, 3%) and used 0% salinity as a control to explore the response of the CW-MFC system to the salinity gradients, laying a foundation for the future extension of the salinity range to higher levels. The research results obtained can deepen the intrinsic connection between salinity and performance and provide reference and prediction directions for a wider range of salinity conditions, enabling the CW-MFC system to better adapt to the actual working conditions of higher concentrations, diversification, and complexity, and providing valuable schemes and ideas.

Table 1. Artificial simulation of the composition of brine from seawater desalination.

Ingredient	Concentration (mg/L)	Ingredient	Concentration (mg/L)
$C_6H_{12}O_6$	208	$MgSO_4{\cdot}7H_2O$	200
$(NH_4)_2SO_4$	56.604	$CaCl_2$	15
KNO_3	75.75	$FeCl_3{\cdot}6H_2O$	1
KH_2PO_4	4.34	$MnSO_4{\cdot}H_2O$	28
$NaHCO_3$	196	$CoCl_2{\cdot}6H_2O$	0.24
KBr	98	$Na_2MoO_4{\cdot}2H_2O$	0.04
H_3BO_3	26	$ZnSO_4{\cdot}7H_2O$	0.12

2.2. Screening Methodology for Salt-Tolerant Plants

The key to treating concentrated brine from seawater desalination using CW-MFC lies in screening out plants with physiological tolerance to salt and the ability to remove pollutants. Through a literature review, three salt-tolerant plants commonly used in constructed wetlands for treating saline wastewater were selected: Phragmites australis, Suaeda salsa, and Bruguiera gymnorrhiza as experimental plants, and their salt tolerance levels, water purification capabilities, and growth conditions were compared. The experiment was carried out in a pot-culture manner. Seedlings of the same variety with basically the same growth were selected and placed in large plastic pots with a height of 20 cm and a diameter of 50 cm. Garden soil was used as the cultivation substrate for the salt stress test. The laboratory temperature was controlled at 20–25 °C. Artificially simulated concentrated brine from seawater desalination (the water sample composition is shown in Table 1) was used as the culture solution. At the beginning of the experiment, the water surface height was close to the rim of the pot, and domestication was carried out for 27 days. During the experiment, a gradient salt addition method was adopted, with the salt concentration increasing by one gradient every 6 days. The growth of the plants was observed and recorded under salt concentrations of 0%, 1%, 2%, and 3%, and a comparative analysis of the pollutant purification effect was carried out. By observing and recording the growth conditions of the three kinds of plants under different gradient salt stress, suitable, relatively salt-tolerant wetland plants were screened.

2.3. Experimental Setup

In this study, a vertical up-flow CW-MFC system was constructed (as shown in Figure 1). The reactor of the device is made of plexiglass. It has an inner diameter of 180 mm, a height of 520 mm, and a total volume of 13.23 L. The effective water output is 5.15 ± 0.1 L. The dimensions of the filler inside the reaction device are shown in Table 2.

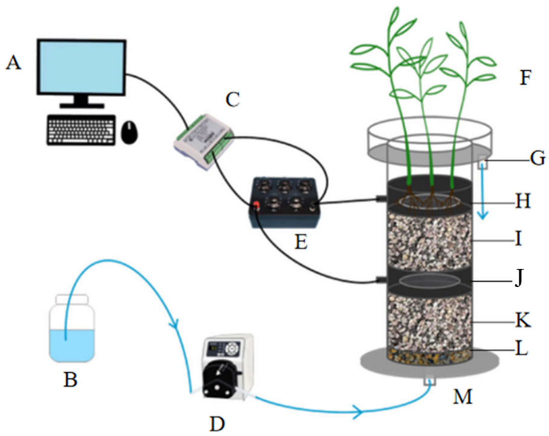

Figure 1. Schematic diagram of the CW-MFC. (A) Computer; (B) wastewater tank; (C) current collector; (D) peristaltic pump; (E) variable-resistance box; (F) wetland plants; (G) filtered effluent; (H) cathode layer; (I) intermediate fillers; (J) anode layer; (K) lower fillers; (L) pebble support layer; (M) wastewater influent.

Table 2. Table of the sizes and details of the filler inside the reactor device.

Section	Filter	Height (mm)	Particle Size and Details (mm)
H	Activated cathode layer	30	4–6
I	Intermediate fillers	180	Bio-ceramsite: zeolite = 1:1
J	Activated anode layer	80	3–5
K	Lower fillers	180	Bio-ceramsite: zeolite = 1:1
L	Pebble support layer	80	3–5

In this device, the sludge from the aerobic tank of the Sapphire Water Sewage Treatment Plant in Changle County was inoculated in the cathode area, and the anaerobic granular sludge from the anaerobic tank of the Sewage Treatment Station of Weifang Insoon Industrial Company was inoculated in the anode area. After the activated sludge was aerobically and anaerobically cultured for one week, respectively, under laboratory conditions, 1 L of it was pumped into the activated carbon particle areas of the cathode and anode, respectively. Based on the plant screening results, Bruguiera gymnorrhiza (F) was transplanted to the cathode of the CW-MFC device, and its roots were distributed in the cathode layer to facilitate the effective exchange of oxygen between the atmosphere and the roots. The experimental device was placed beside the indoor window to ensure 8 h of sunlight exposure.

A stainless-steel mesh (12 meshes, with a diameter of 180 mm and a height of 50 mm) was buried between the anode layer and the cathode layer as a current collector to facilitate electrical conduction, and it was connected to the external circuit by copper-core wires. A variable-resistance box, E, was set in the external circuit as an external resistance, and the resistance value was set to 1000 Ω. The changes in current and voltage of the reactor were transmitted to the computer A through the current collector C for recording.

The artificially prepared concentrated brine from seawater desalination in wastewater tank B was continuously pumped by the peristaltic pump D from the bottom into the device. Then it overflowed from the upper layer of the device and flowed out as filtered effluent through port G. The hydraulic retention time was three days. The air-conditioning system in the laboratory maintained the room temperature between 23 and 27 °C.

On the basis of the basic reactor device (Figure 1) and the planting of the salt-tolerant plant Bruguiera gymnorrhiza, three sets of devices were set up: the planted closed-circuit (P-CW-MFC), the non-planted closed-circuit (NP-CW-MFC), and the planted open-circuit (OP-CW-MFC). The entire cycle lasted 61 days. By changing the influent salinity (0%, 1%, 2%, 3%), the impact of salinity on the efficiency of the CW-MFC system was explored. After the system achieved stable power generation, the water quality was measured, and the entire cycle lasted 80 days. And under the condition of 1% influent salinity, the influence of electrode spacing and hydraulic retention time on the system efficiency was investigated.

2.4. Analytical Methods

Since the salinity of the influent water is set to four levels: 0%, 1%, 2%, and 3%, the measurement methods for relevant water quality indicators are divided into two parts: fresh water and concentrated brine. The water quality indicators and analysis methods selected in this paper are shown in Table 3. TDS is measured using a portable conductivity meter (LeiciDDBJ-350, Shanghai, China).

Table 3. Water quality analytical methods.

Water Quality Indicators	Salinity	Method
COD	0%	Dichromate method
	1–3%	Alkaline potassium permanganate method
NH_4^+-N	0%	Nessler's reagent spectrophotometry
	1–3%	Sodium hypobromite oxidation method
TN	0%	Alkaline potassium persulfate digestion–ultraviolet spectrophotometry
	1–3%	Alkaline potassium persulfate oxidation method
TP	0%	Ammonium molybdate spectrophotometry
	1–3%	Potassium persulfate oxidation method

The output voltage of CW-MFC is automatically collected by the data-acquisition card at both ends of the external resistor every 5 min and stored in the computer to reflect the power-generation situation. The voltage was measured every day during the experiment, and the influent and effluent water samples were collected and measured every 3 days.

The polarization curve and power density curve, two important parameters of the power-generation performance, are obtained. The former is drawn with current density as the abscissa and electrode potential as the ordinate by adjusting the external-resistance value (10–105Ω) during stable power generation with the potentiostatic method to record the stable voltage value for anode and cathode polarization curves. The latter is plotted with current density as the abscissa and power density as the ordinate.

At the end of the period of operation, the surface characteristics of electrodes was characterized by field emission scanning electron microscopy (JSM-7800F Prime, Tokyo, Japan). At the same time, the microbes acclimated on the substrate surface at the targeted locations were carefully removed and immediately stored in sterilized centrifuge tubes at −20 °C, before further processing. The biofilm attached to the surface of the respective substrates was used for microbial diversity analysis and the total genome DNA [29]. For microbial community analysis, the V3–V4 region of the 16S rRNA gene was amplified using specific primers and sequenced by an Illumina MiSeq PE300 platform. Library construction was carried out using the TruSeq Nano DNA LT Library Prep Kit from Illumina (San Diego, CA, USA). After the library passed the quality inspection, sequencing was performed on the Miseq PE300 platform of Illumina Miseq.

The testing methods and data described in this study were all obtained from the measurements carried out after the CW-MFC system reached a fully stable operating state. The effluent data showed stability, and the test results were reproducible and reliable.

3. Discussion

3.1. Screening of Salt-Tolerant Plants

The growth conditions of the three plants in different salinity environments are shown in Table 4. It can be concluded from the table that at 1% salinity, all three plants have good adaptability and grow normally, with an increase in plant height. When the salinity increases to 2%, the leaves of the reed start to turn yellow and wilt, and it hardly grows. The plant becomes soft and tilts. However, Suaeda salsa and Bruguiera gymnorrhiza still grow normally, with new buds emerging. At 3% salinity, the leaves of the reed turn completely yellow, and its roots rot and wither successively until it dies completely. Suaeda salsa hardly grows, and the growth of Bruguiera gymnorrhiza slows down, indicating that Bruguiera gymnorrhiza has better adaptability than Suaeda salsa at 3% salinity. The salt tolerance of wetland plants from strong to weak is in the order of Bruguiera gymnorrhiza > Suaeda salsa > Phragmites. Therefore, Bruguiera gymnorrhiza was selected as the wetland plant to be planted in this study.

Table 4. Changes in characteristics of three plant species under different salt stress.

Salinity	Phragmites	Suaeda Salsa	Bruguiera Gymnorrhiza
0%	Grow normally with new leaves	Grow normally with new leaves	Grow normally with new leaves
1%	Grow normally with new leaves	Grow normally with new leaves	Grow normally with new leaves
2%	The leaves turn yellow and the plants wilt	Grow normally with new leaves	Grow normally with new leaves
3%	All the leaves have turned completely yellow and the plants have withered and toppled over	It hardly grows at all	Grow slowly

3.2. The Role of Plants in the CW-MFC System

The influence of planting Bruguiera gymnorrhiza on the performance of the CW-MFC system is shown in Figure 2.

The plant conditions after 60 days of CW-MFC operation are shown in Figure 2d. The plant sizes in different salinity systems are basically the same; the plants grow well, and the leaf colors are normal, indicating that Bruguiera gymnorrhiza has salt tolerance and can be used in the CW-MFC system.

It is found that the removal rate of P-CW-MFC is the highest (84.8%), and the removal rate of OP-CW-MFC is the lowest (78.41%), indicating that the current effect has an obvious promoting effect on COD removal, the oxidative catalysis of the anode biofilm is strong, and the COD removal rate of the system is high, which is consistent with the research results of Xu et al. [30]. The removal rate of NP-CW-MFC is 81.65%, lower than that of the P-CW-MFC system, suggesting that plants have a promoting effect on the COD removal of CW-MFC. This is because under salt stress, plants will increase root exudates to provide energy for microorganisms [31], root exudates will increase electron-related substances in the cathode and anode regions [32], and provide a favorable environment for microorganisms [33], etc., thus improving the performance of the system.

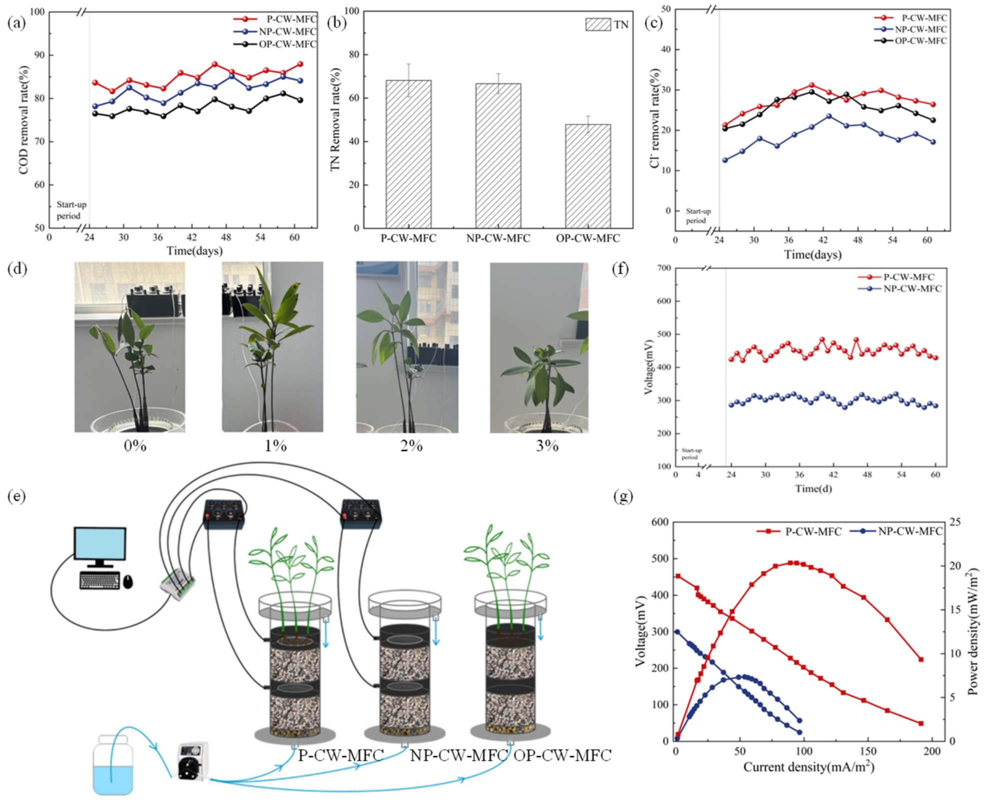

Figure 2. Influence of plants on the performance of CW-MFC systems: (**a**) COD removal rate, (**b**) TN removal rate, (**c**) Cl^- removal rate, (**d**) growth situation of Bruguiera gymnorrhiza in water with different salinities, (**e**) schematic diagram of the experimental apparatus, (**f**) system output voltage, (**g**) system polarization curve and current density.

Figure 2b shows the removal situation of total nitrogen (TN) in the system. The total nitrogen removal rates of P-CW-MFC and NP-CW-MFC are 68.12% and 47.856%, respectively, indicating that planting plants can increase the total nitrogen removal rate. Through further analysis of the saline water composition and measurement of the content of different forms of nitrogen at the plant root area of the cathode, it is found that nitrate nitrogen (NO_3^--N) is the dominant nitrogen form, accounting for 73.421% of the total nitrogen. Plants absorb nitrate nitrogen through their roots and assimilate it into their own organic nitrogen compounds. Meanwhile, some substances secreted by plant roots also provide a suitable living environment for microorganisms, significantly promoting the denitrification process of microorganisms and enabling more nitrate nitrogen to be converted into nitrogen gas and escape from the system [34]. The synergistic effect of these two aspects has a relatively obvious promoting effect on the total nitrogen removal. The total nitrogen removal rate of OP-CW-MFC is 66.637%, which is not much different from that of P-CW-MFC, meaning that the total nitrogen removal rate has nothing to do with whether the microbial battery circuit is connected or not.

Under the condition of 1% salinity in the influent (as shown in Figure 2c), in terms of the removal effect of chloride ions (Cl−), several devices such as P-CW-MFC, NP-CW-MFC, and OP-CW-MFC exhibited different performances. Their average treatment efficiencies were 29.96%, 17.42%, and 25.71%, respectively. It can be seen that the microbial fuel cells with plants showed a more prominent effect in removing chloride ions.

From the perspective of the mechanism of chloride ions entering plants, Cl− in water mainly enter the plant body through the plant root system. The plant root system has two ways of transporting ions. One is the passive ion transport channel. When the chloride ion concentration in the external environment is relatively high, chloride ions can enter the cells smoothly from the outside along the concentration gradient through these channels. The other is the active transport mechanism. When the chloride ion concentration is relatively low, the plant will consume energy to drive transporter proteins to achieve the absorption of chloride ions. $Cl-$ that enter the plant body will then be transported inside the plant. With the help of the transpiration stream, they can be transported to various organs, such as the stems and leaves of the plant, and continuously accumulate within the plant. Moreover, this accumulation will not hinder the growth of the plant but can provide necessary elements for the growth of the plant, which further promotes the removal of chloride ions in high-salinity water. At the same time, the wetland substrate itself has a certain adsorption effect and can play a role in adsorbing and removing chloride ions. The existence of plants greatly enhances the efficiency of the entire removal process. Therefore, the microbial fuel cell device with plants shows a better effect in removing chloride ions in concentrated salt water.

In terms of electricity generation performance (as shown in Figure 2f,g), there were differences in the output voltage and maximum power density between P-CW-MFC and NP-CW-MFC under 1% salinity. The output voltage of P-CW-MFC was 34.1% higher than that of NP-CW-MFC, and the maximum power density was 64.79% higher. The reasons include that plants provide a favorable environment for microorganisms [35], increase the abundance and activity of microorganisms [36], and relieve the inhibition of microorganisms by high salinity 141. Regarding the internal resistance, the internal resistances of the P-CW-MFC and NP-CW-MFC systems were 96.46 Ω and 119.4 Ω, respectively. The oxygen secretion by plant roots can enhance the redox potential and thereby reduce the internal resistance.

3.3. Comparison of Electricity Generation Performance of CW-MFC in Treating Concentrated Brine from Seawater Desalination

The electricity generation performance of the CW-MFC system in treating concentrated brine with different salinities is shown in Figure 3.

During the water quality monitoring phase, Figure 3a presents the curves of voltage variation over time for each CW-MFC system after stable operation. During the 60-day measurement period, the output voltages of CW-MFC systems with different salinities (0%, 1%, 2%, 3%) exhibited certain patterns. The average output voltages were 382.7 ± 22.3 mV, 436.6 ± 25.2 mV, 617.3 ± 25.7 mV, and 494.3 ± 24.1 mV, respectively. Among them, the output voltage was the highest when the influent salinity was 2% and the lowest when it was 0%. In the salinity range of 0–2%, the output voltage increased with the increase in salinity, which was consistent with the research of Xu et al. [37], indicating that an appropriate increase in salinity can improve the electron transfer rate, probably by increasing the conductivity or ionic strength of the saline wastewater to promote the electricity generation process. However, when the salinity increased to 3%, the voltage decreased, which was in line with the research results of Xin et al. [38]. Excessive salinity can cause dehydration of anode microorganisms and slow down the electron transfer rate [39].

Regarding the polarization density curve and power density curve (Figure 3b–e), curves under different salinities were drawn after the system was stably operated. The maximum power densities (PAmax) of the four-group devices were 6.04 mW/m^2, 16.63 mW/m^2, 45.83 mW/m^2, and 38.71 mW/m^2, respectively. The PAmax of the 2% salinity system was the highest, which was 6.64 times higher than that of the 0% salinity system. The PAmax of the 3% salinity system was 15.5% lower than that of the 2% salinity system. This was consistent with the results of Xin et al. in treating saline wastewater with MFC, indicating that the electricity generation performance was the best at 2% salinity.

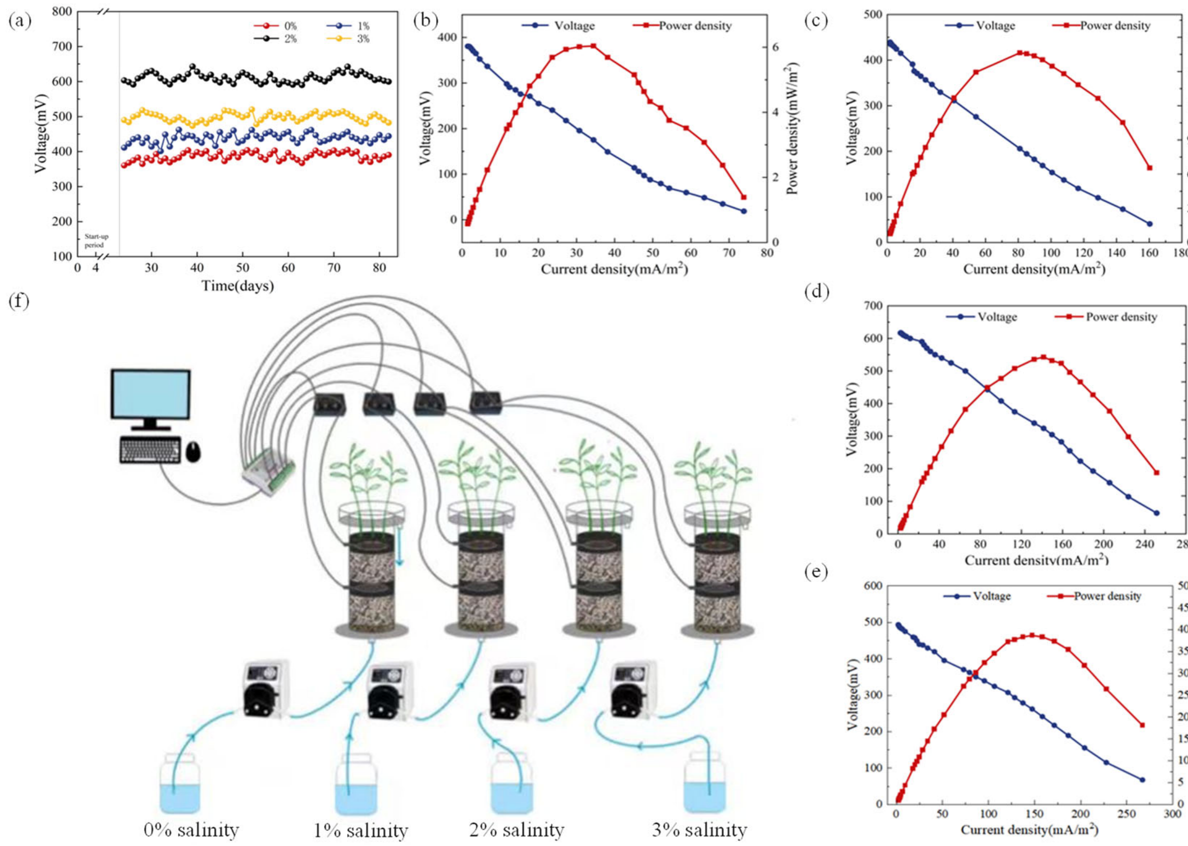

Figure 3. Electricity generation performance of the CW-MFC system, (**a**) output voltage, polarization curve, and power density of the inlet system at (**b**) 0% salinity, (**c**) 1% salinity, (**d**) 2% salinity, (**e**) 3% salinity, (**f**) schematic diagram of the influent device with different salinities.

In addition, internal resistance data were obtained by fitting the linear region of the polarization curve. The internal resistances of the four CW-MFC systems were 231.52 Ω, 103.17 Ω, 85.63 Ω, and 70.41 Ω, respectively. The increase in salinity can reduce the internal resistance, which was consistent with the research of Olivier et al. An appropriate increase in salinity can increase the solution conductivity and reduce the internal resistance, which is beneficial for electrons to transfer from electrochemically active bacteria (EAB) to the electrode [40]. However, excessive salinity will inhibit the enzyme activity of EAB and reduce the electricity generation performance [41]. To sum up, the optimal salinity condition for electricity generation of the CW-MFC system in this study is 2%.

3.4. Comparison of Water Purification Performance of CW-MFC in Treating Concentrated Brine from Seawater Desalination

The pollutant removal efficiencies of the CW-MFC system for concentrated brine with different salinities are shown in Figure 4. The system efficiencies are analyzed and compared by analyzing the removal rates of COD, TN, TDS, and TP.

As shown in Figure 4a, the removal rates are 86.21 ± 2.75%, 85.18 ± 2.45%, 84.15 ± 2.86%, and 83.13 ± 2.34%, respectively. The results indicate that salinities of 1% and above have a slight inhibitory effect on the treatment of organic matter, causing a slight decrease in the COD removal performance. This is because under high-salinity conditions, microorganisms consume energy to generate protection mechanisms for survival. As a result, the energy available for reproduction is reduced, and their growth is slowed down, thereby reducing the COD removal effect. However, in this study, glucose, which is easily degradable [22], is used as the organic carbon source, so that the COD removal rate remains at a relatively high level when the salinity increases, which is consistent with relevant research results.

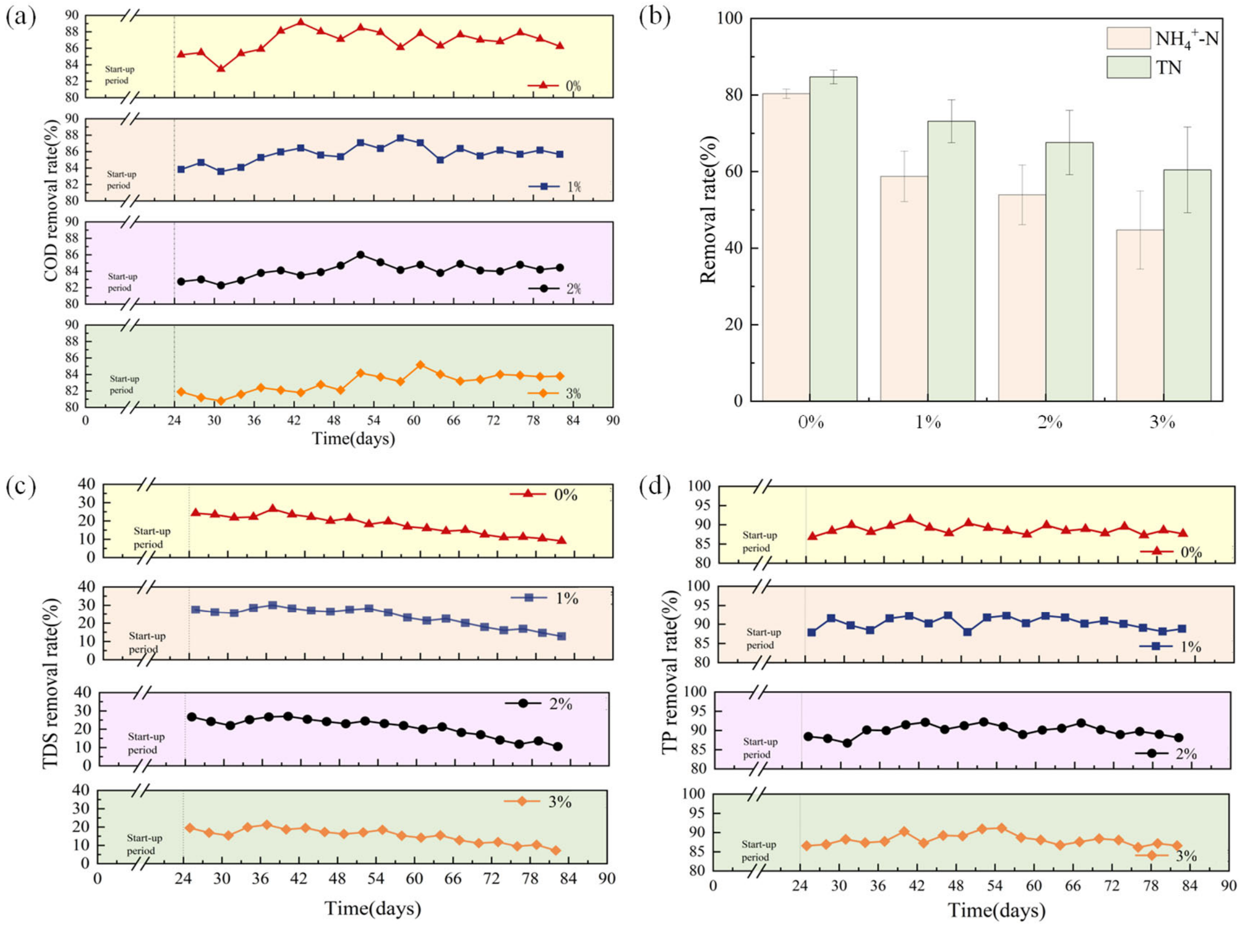

Figure 4. Water purification performance of the CW-MFC system, (**a**) COD removal rate, (**b**) TN removal rate, (**c**) TDS removal rate, (**d**) TP removal rate.

Salinity stress exerts a negative influence, particularly at elevated salinity levels. Regarding the removal rate of ammonium-nitrogen (NH_4^+-N) (as depicted in Figure 4b), it reaches its peak at 80.34% under 0% salinity. Subsequently, this rate declines as the salinity increases. The elevation in salinity inhibits the nitrification process. This occurs because salinity impacts the activities of nitrite-forming bacteria and nitrate-forming bacteria. Specifically, it leads to the accumulation of nitrite and disrupts the nitritation process, thereby reducing the conversion rate of ammonia-nitrogen [42,43].

Upon further analyzing the proportion of each nitrogen form within the total nitrogen (TN), it is found that in the initial influent, ammonium-nitrogen (NH_4^+-N) constitutes approximately 30% of the total nitrogen (TN), nitrate-nitrogen (NO_3^--N) accounts for around 50%, and the remaining 20% exists in the form of organic nitrogen. With the operation of the system and variations in salinity, the proportion of each nitrogen form also undergoes changes.

The trend in the variation of the total nitrogen (TN) removal rate is comparable to that of ammonium-nitrogen (NH_4^+-N), although the TN removal rate is relatively higher. The reasons for this are twofold. Firstly, nitrifying bacteria are highly sensitive to salinity shocks [44]. When salinity rises, the nitrification process becomes restricted. Secondly, the aerobic-anaerobic mixed environment created by the constructed wetland–microbial fuel cell (CW-MFC) system is conducive to denitrification. Microbial communities play a crucial role in the denitrification process, mainly by gradually reducing nitrate-nitrogen to nitrogen gas and then discharging it from the system. The amount of nitrate-nitrogen removed through microbial denitrification accounts for approximately 40% of the total nitrogen removal amount.

Simultaneously, plants also contribute significantly to nitrogen removal. Plant roots primarily absorb ammonium-nitrogen and nitrate-nitrogen. Through an analysis of the changes in nitrogen content within plants, it has been determined that the total amount of ammonium-nitrogen and nitrate-nitrogen absorbed by plants constitutes around 30% of the total nitrogen removal amount. Plants assimilate these absorbed nitrogens into their own organic nitrogen compounds for growth, metabolism, and other processes. Nevertheless, excessive salinity can suppress plant growth, which in turn affects the nitrogen-absorption efficiency of plants and the overall nitrogen-removal efficiency of the system [45,46].

Figure 4d illustrates that the CW-MFC system demonstrates a favorable total phosphorus (TP) removal effect under different salinities. The removal rates are all above 85%, and the differences among them are not substantial. Salinity has a minimal impact on it. The slightly higher removal rate at 1% salinity might be associated with the optimal growth salinity of plants. The phosphorus removal mechanism of the system mainly encompasses plant absorption, microbial assimilation, and filter media substrate restoration. Based on the experimental data, it can be inferred that different salinities do have certain effects on the growth and metabolism of microorganisms as well as the growth of plants. However, the change in the total phosphorus removal rate of the system is not significant, suggesting that the primary phosphorus removal mechanism within the system is the adsorption effect of the wetland filter media, which aligns with previous studies.

In the RO seawater desalination method, only 40–50% of the water can permeate the reverse osmosis membrane to form desalinated water. The remaining 50–60% of the water will contain over 99% of the dissolved substances in the original seawater, resulting in this portion of water having higher total dissolved solids (TDS), which is generally 1.5–2 times that of the original seawater. As shown in Figure 4c, the CW-MFC exhibits a certain removal rate of TDS under different salinities. The salinity corresponding to the maximum removal rate coincides with the optimal growth salinity of plants, indicating that plants play a dominant role in TDS removal [47]. However, as the experiment progresses, the TDS removal efficiency of each system decreases. This might be due to the blockage of the filler pores, suggesting that the filler also contributes to the TDS removal. In summary, different salinities have varying degrees of impact on the pollutant removal efficiency of the CW-MFC system, which is in line with relevant research results [48].

3.5. Effect of Salinity Stress on the Microbial Community in CW-MFC

We further investigated the growth of the microbial community in the electrode area when CW-MFC treats concentrated brine from seawater desalination and compared the differences between the initial sludge and the microbial community after treating concentrated brine. The microbial population structure and scanning electron microscope images are shown in Figure 5. In this study, the initial sludge was used as the control group (BG), and low salinity (1%) and high salinity (3%) were used as the experimental groups. High-throughput sequencing was performed on the substrate microorganisms in the anode and cathode areas of the CW-MFC system. Samples from each area were named BG-A (control group-anode), BG-C (control group-cathode), L-CM-A (low-salinity CW-MFC-anode), L-CM-C (low-salinity CW-MFC-cathode), H-CM-A (high-salinity CW-MFC-anode), and H-CM-C (high-salinity CW-MFC-cathode), respectively.

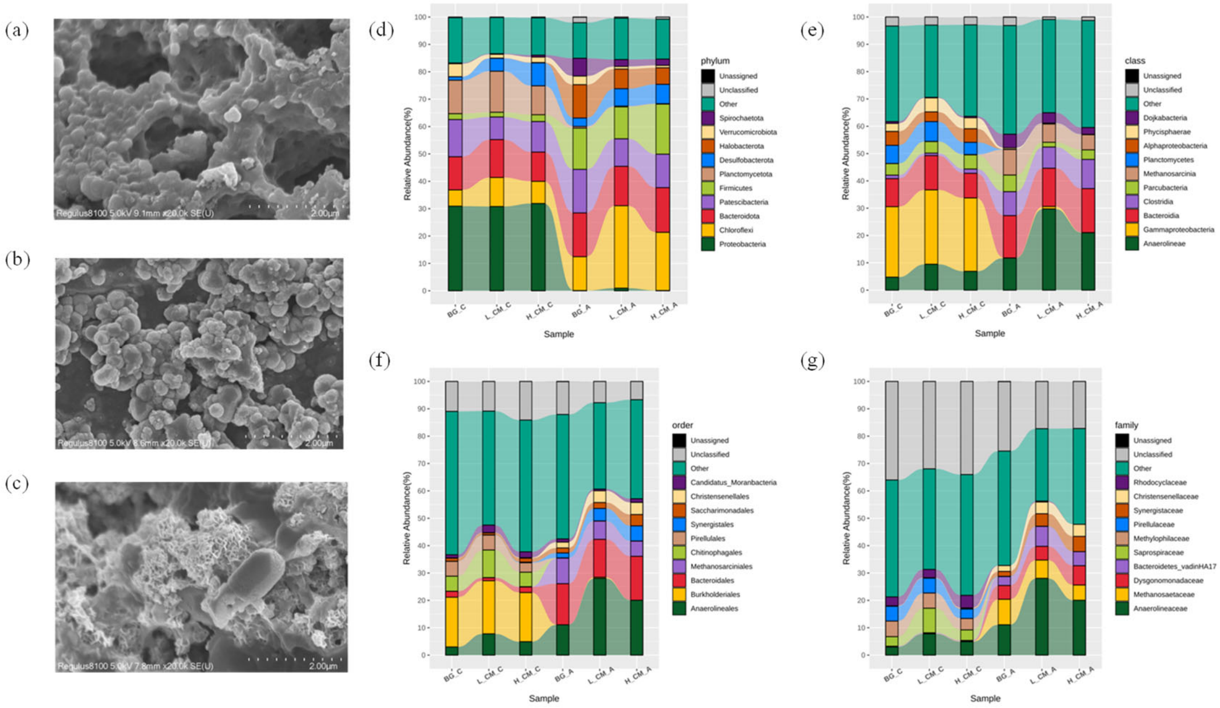

Figure 5. Micro-structure and microbial community, (**a**) the surface of activated carbon particles before biofilm formation, (**b**) the biofilm on the surface of activated carbon particles at the anode, (**c**) the biofilm on the surface of activated carbon particles at the cathode, relative abundance of microbial community at the levels of (**d**) phylum, (**e**) class, (**f**) order, and (**g**) family.

Upon comparing Figure 4a with Figure 4b,c, it becomes evident that significant alterations have taken place on the surface of the activated carbon. The attachment and growth of microorganisms on the surface of the activated carbon can be clearly observed. In Figure 4b, it is noticeable that the microorganisms attached to the anode surface are spherical bacteria, which aggregate into clusters and entirely cover the surface of the activated carbon, thereby forming a stable biofilm structure. Meanwhile, in Figure 4c, it can be seen that the microorganisms attached to the cathode surface are rod-shaped bacteria. It is worth noting that the microorganisms on the surfaces of the activated carbon particles at both the anode and cathode thrive well under salinity stress, thus guaranteeing the pollutant treatment and power generation capabilities of the CW-MFC system.

Proteobacteria and Chloroflexi account for relatively high proportions in each sample. In the anode region, Chloroflexi gets enriched and grows vigorously under low-salinity conditions (L-CM-A). Although its growth is somewhat inhibited under high-salinity conditions (H-CM-A), its abundance remains higher than that of the initial sludge (BG-A). This microorganism has the ability to decompose substances and conduct autotrophic denitrification, which is conducive to enhancing the pollutant treatment efficiency [49]. In the cathode region, Proteobacteria maintains a relatively stable proportion and plays a crucial role in degrading nutrients and organic pollutants, as well as in bio-electricity production. The abundances of Bacteroidetes and Firmicutes in the anode are higher than those in the cathode. Both of these belong to electrochemically active bacteria (EAB) [50,51]. Moreover, the abundance of Desulfobacterota is higher under high-salinity conditions in the anode [52]. The CW-MFC system can enrich it to facilitate electricity generation. By comparing the sum of the relative abundances of the three typical EAB phyla, it is found that the high-salinity CW-MFC system has the highest value in the anode region, which elucidates why this system can generate more electrical energy.

Among the various microbial groups, Anaerolineae and Gammaproteobacteria exhibit the highest abundances. In the anode, Anaerolineae is capable of decomposing organic matter, and its abundance in different-salinity CW-MFC systems surpasses that of the initial sludge. Its abundance initially increases and then decreases as the salinity rises. In each anode sample, the abundance of Bacteroidia exceeds 14%. In the cathode, it is mainly composed of Gammaproteobacteria and Bacteroidia. The abundance of Clostridia in the CW-MFC anode increases in tandem with the elevation of salinity.

Anaerolineales, Burkholderiales, and Bacteroidales are present in the highest abundances. Anaerolineales can adapt to changes in salinity and are more abundant under low-salinity conditions. The CW-MFC system promotes an increase in its abundance, which is beneficial for the degradation of organic matter. The proportion of Bacteroidales in the anode is higher than that in the cathode. The combined abundances of these groups under different salinities play a dominant role, indicating that the EAB in the anode region gradually becomes enriched and emerges as the dominant strain under the influence of the system's domestication.

Furthermore, dominant bacterial families are detected in both the anode and cathode. For instance, the proportion of Anaerolineaceae in the anode is higher than that in the cathode. This family possesses the function of degrading carbohydrates and cellular materials. Similarly, the proportion of Bacteroidetes_vadinHA17 in the anode is also higher than that in the cathode, and it is capable of degrading refractory organic matter. The abundances of these dominant bacterial families first increase and then decrease with the increase in influent salinity. Notably, their abundances in the CW-MFC system are all higher than those in the initial sludge. These variations within the microbial community have a profound impact on the performance of the CW-MFC system.

3.6. Operation Performance Optimization of the CW-MFC System

The distance between the anode and cathode in the CW-MFC system is a key variable. If it is too small, it is not conducive to the diffusion of ionic gases, and if it is too large, the power generation performance will decline. The hydraulic retention time (HRT) determines the reaction and contact time of pollutants in the device. In this study, under 1% salinity, the electrode spacing between the anode and cathode and different HRTs were changed. The purification effect on concentrated brine and power generation performance of the CW-MFC system under different operating conditions were compared, as shown in Figure 6.

Figure 6a,b delineates the influence exerted by the electrode spacing on the water purification and electrical performance within the CW-MFC system. Under a salinity regime of 1%, fluctuations in the electrode spacing precipitate corresponding variations in the removal efficiencies of chemical oxygen demand (COD) and total nitrogen (TN), as well as the power generation capabilities of the CW-MFC. With respect to the removal rates of COD and TN, when the electrode spacing is configured at 5 cm, 10 cm, and 15 cm, the mean removal rates of COD are recorded as 83.47%, 85.96%, and 82.6% respectively, while the mean removal rates of TN are 60.13%, 69.46%, and 65.47% in tandem. Notably, the peak removal rates for both COD and TN are attained when the electrode spacing is set at 10 cm.

This phenomenon can be ascribed to the fact that small-molecule glucose is amenable to facile degradation, and this specific salinity level imposes a negligible inhibitory effect on the microorganisms implicated in COD remediation. However, the electrode spacing assumes a pivotal role in mass transfer kinetics. In the event that the spacing is overly constricted, the dissolved oxygen concentration in the anode region will experience an augmentation, while the potential difference will concomitantly diminish. Such a scenario is inimical to the progression of electrochemical reactions and the abatement of organic matter. Conversely, if the spacing is excessively expansive, the proton mass transfer rate will be detrimentally affected [11]. Concurrently, a relatively diminutive spacing elongates the distance from the inlet to the anode, and the ensuing alteration in organic matter consumption exerts an impact on the proliferation of microorganisms and the denitrification reaction [53], which is congruent with the research findings of Mou et al. [21]. From the vantage point of power generation performance, under a 1% salinity condition, when the electrode spacing is 5 cm, 10 cm, and 15 cm, the average voltages are measured as 385.77 mV, 426.49 mV, and 360.37 mV, respectively, with the maximum output voltage of 471.53 mV being registered at 10 cm. The output voltage initially ascends and subsequently declines. Significantly, the internal resistance and the maximum power density undergo pronounced alterations with varying electrode spacings. As the spacing augments, the internal resistance also escalates, while the power density initially increases and then decreases. If the spacing is too narrow, the organic matter will not be thoroughly degraded, thereby impinging on the cathode reaction and power generation. On the other hand, if the spacing is too wide, the proton mass transfer will be retarded, leading to an elevation in internal resistance and a subsequent diminution in power density, which is in accord with the research outcomes of Wang et al. [54].

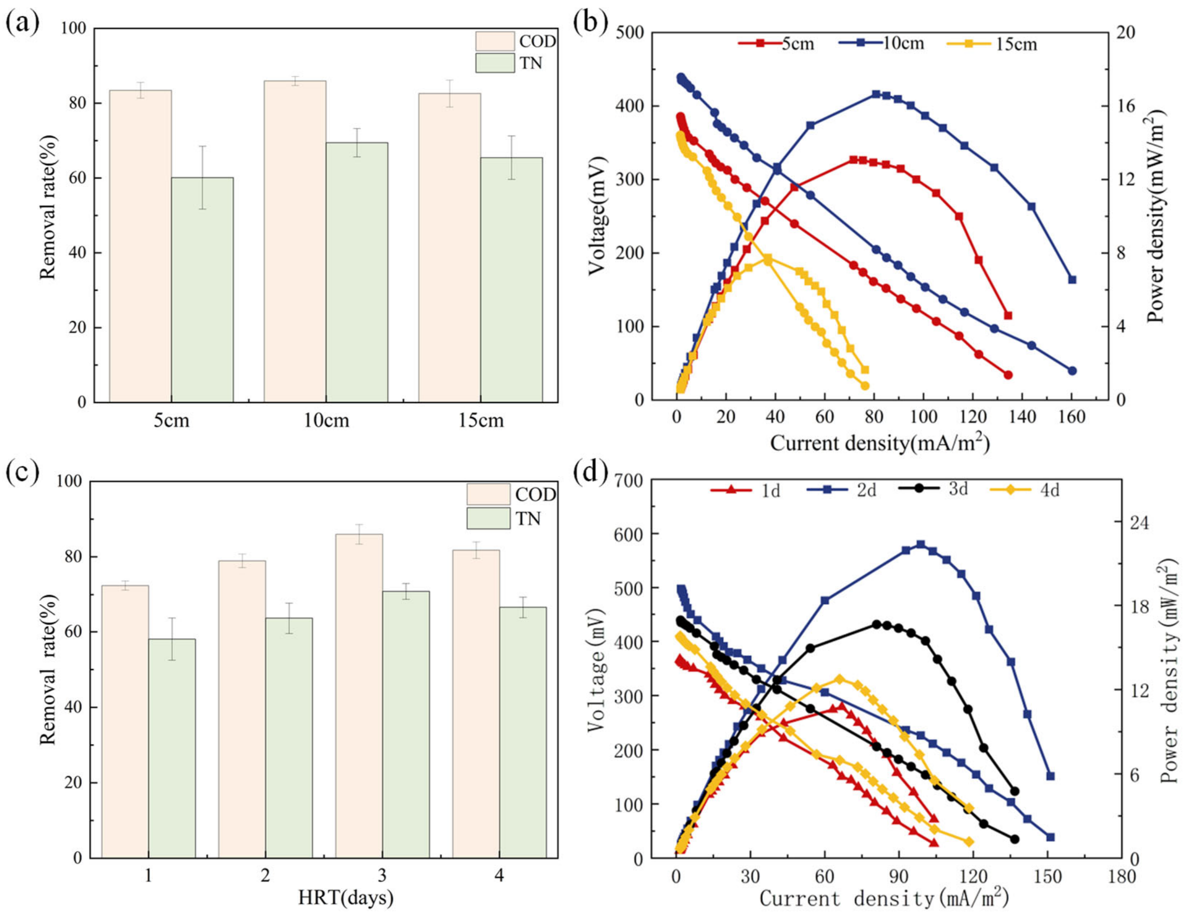

Figure 6. Influence of electrode spacing and HRT on system efficiency, (**a**) relationship between water purification efficiency and electrode spacing, (**b**) relationship between polarization curve, power density, and electrode spacing, (**c**) relationship between water purification efficiency and HRT, (**d**) relationship between polarization curve, power density, and HRT.

Figure 6c,d portray the impact of hydraulic retention time (HRT) on the performance of the CW-MFC system. Under a 1% salinity level and with an electrode spacing of 10 cm, when the HRT is varied within the range of 1 to 4 days, the removal rates of COD and TN both initially exhibit an upward trend and subsequently decline. The maximum COD removal rate is achieved when the HRT is 3 days (85.96%), and the maximum TN removal rate occurs when the HRT is also 3 days (70.84%). A relatively abbreviated HRT culminates in incomplete reactions between microorganisms and organic matter, as well as inadequate denitrification [55]. Conversely, an overly protracted HRT engenders greater consumption of bottom-layer organic matter, a reduction in microbial activity, and an intensification of the anaerobic environment, all of which are unfavorable for nitrification and the aerobic degradation of organic matter. In terms of power generation performance, under a 1% salinity condition, as the HRT is incremented from 1 day to 4 days, the power generation performance initially ameliorates and then deteriorates, reaching its zenith when the HRT is 2 days. A short HRT induces incomplete degradation of organic matter, which in turn affects the cathode potential and power generation. Appropriate elongation of the HRT can enhance power generation performance [56], but an excessively long HRT will cause the internal resistance to rise and the output voltage to decline due to insufficient anode nutrients. In summation, under a 1% salinity condition, the optimal electrode spacing is determined to be 10 cm. The optimal HRT for TN treatment is 3 days, and considering power generation performance, the optimal HRT is 2 days.

4. Conclusions

This paper studies the treatment of concentrated brine from seawater desalination with different concentrations by the CW-MFC system. The results indicate that Bruguiera gymnorrhiza has a strong salt tolerance, grows well in the CW-MFC system, and has a positive impact on the system's performance. When the salinity is less than 2%, the power generation performance of the system improves with the increase in salinity. When the salinity is greater than 2%, the increase in salinity will inhibit the power generation of the system, and the power generation effect is the best at 2% salinity. As the salinity rises, the internal resistance of the system has been decreasing, and the removal of chemical oxygen demand (COD) and nitrogen is inhibited. The removal of total phosphorus (TP) is less affected by salinity. Plants play a major role in the removal of total dissolved solids (TDS). Under salinity stress, the structure of the microbial community changes, but the microorganisms grow well. When the electrode spacing is 10 cm, both the power generation performance and the pollutant treatment capacity are optimal, and the optimal hydraulic retention time is 2 days. This study successfully reveals the internal relationship between the change of salinity gradient and the performance of the system, provides theoretical support and prediction directions for the application of the CW-MFC system under a wider range of salinity conditions, promotes the effective application of the system in actual working conditions, and provides valuable schemes and ideas for its optimization and development. In the future, it is necessary to conduct in-depth research on the growth and reproduction of microorganisms and the electron transfer mechanism, the electrochemical structure of the system, and the degradation of substances.

Author Contributions: L.W. (Li Wang), X.H. and Y.Z. have the same contribution; L.W. (Li Wang) is the corresponding author; conceptualization, L.W. (Lin Wang); data curation, X.H. and Y.Z.; formal analysis, X.H. and Y.Z.; funding acquisition, L.W. (Li Wang); investigation, Y.Z.; methodology, L.W. (Li Wang) and Y.Z.; project administration, L.W. (Lin Wang); resources, L.W. (Li Wang); supervision, L.W. (Li Wang); validation, J.W.; visualization, Y.Z. and J.W.; writing—original draft, X.H. All authors have read and agreed to the published version of the manuscript.

Funding: This study was supported by the National Key Research and Development Program of China (Grant NO. 2018YFC0408000. 2018YFC0408004).

Data Availability Statement: Data will be made available on request.

Conflicts of Interest: The authors declare that they have no known competing for financial interest or personal relationships that could have appeared to influence the work reported in this paper.

References

1. Ayaz, M.; Namazi, M.A.; Din, M.A.U.; Ershath, M.I.M.; Mansour, A.; Aggoune, E.-H.M. Sustainable seawater desalination: Current status, environmental implications and future expectations. *Desalination* **2022**, *540*, 116022. [CrossRef]
2. Zhang, L.; Li, X.; Zhong, Y.; Leroy, A.; Xu, Z.; Zhao, L.; Wang, E.N. Highly efficient and salt rejecting solar evaporation via a wick-free confined water layer. *Nat. Commun.* **2022**, *13*, 849. [CrossRef] [PubMed]
3. Mito, M.T.; Ma, X.; Albuflasa, H.; Davies, P.A. Reverse osmosis (RO) membrane desalination driven by wind and solar photovoltaic (PV) energy: State of the art and challenges for large-scale implementation. *Renew. Sustain. Energy Rev.* **2019**, *112*, 669–685. [CrossRef]
4. Clark, G.F.; Knott, N.A.; Miller, B.M.; Kelaher, B.P.; Coleman, M.A.; Ushiama, S.; Johnston, E.L. First large-scale ecological impact study of desalination outfall reveals trade-offs in effects of hypersalinity and hydrodynamics. *Water Res.* **2018**, *145*, 757–768. [CrossRef]
5. Arafat, H.A. *Desalination Sustainability: A Technical, Socioeconomic, and Environmental Approach*; Elsevier: Amsterdam, The Netherlands, 2017.
6. Wang, W.; Huang, X.; Qiu, Y.; Ju, Q.; Zhao, W.; Zhang, X.; Li, Y.; Lei, G.; Liu, C. Index evaluation method for intelligent water regulation management system for water conservancy structure, involves designing evaluation index system of intelligent management body according to judging matrix and set evaluation index weight. CN Patent 117114497-A, 24 November 2023.
7. Ji, B.; Zhao, Y.; Vymazal, J.; Mander, U.; Lust, R.; Tang, C. Mapping the field of constructed wetland-microbial fuel cell: A review and bibliometric analysis. *Chemosphere* **2021**, *262*, 128366. [CrossRef]
8. Ding, X.; Fan, Y.; Zhang, Z.; Chen, D.; Yao, S. Lattice Boltzmann simulation of ion transport during the charging process of porous electrodes in randomly reconstructed seawater desalination batteries. *Int. Commun. Heat Mass Transf.* **2024**, *159*, 107942. [CrossRef]
9. Wu, S.; Lyu, T.; Zhao, Y.; Vymazal, J.; Arias, C.A.; Brix, H. Rethinking Intensification of Constructed Wetlands as a Green Eco-Technology for Wastewater Treatment. *Environ. Sci. Technol.* **2018**, *52*, 1693–1694. [CrossRef]
10. Wang, M.; Zhang, D.Q.; Dong, J.W.; Tan, S.K. Constructed wetlands for wastewater treatment in cold climate—A review. *J. Environ. Sci.* **2017**, *57*, 293–311. [CrossRef]
11. Gupta, S.; Srivastava, P.; Patil, S.A.; Yadav, A.K. A comprehensive review on emerging constructed wetland coupled microbial fuel cell technology: Potential applications and challenges. *Bioresour. Technol.* **2021**, *320*, 124376. [CrossRef]
12. Ramírez-Vargas, C.A.; Arias, C.A.; Zhang, L.; Brix, H. Microbial Community Function in Electroactive Biofilm-based Constructed Wetlands. *Biogeosci. Discuss.* **2018**, *2018*, 1–28. [CrossRef]
13. Abou-Elela, S.I.; Golinielli, G.; Abou-Taleb, E.M.; Hellal, M.S. Municipal wastewater treatment in horizontal and vertical flows constructed wetlands. *Ecol. Eng.* **2013**, *61*, 460–468. [CrossRef]
14. Thalla, A.K.; Chella, D.P.; Anagh, K.; Sony, E. Performance evaluation of horizontal and vertical flow constructed wetlands as tertiary treatment option for secondary effluents. *Appl. Water Sci.* **2019**, *9*, 1–9. [CrossRef]
15. Pandey, M.K.; Jenssen, P.D.; Krogstad, T.; Jonasson, S. Comparison of vertical and horizontal flow planted and unplanted subsurface flow wetlands treating municipal wastewater. *Water Sci. Technol.* **2013**, *68*, 117–123. [CrossRef] [PubMed]
16. Doherty, L.; Zhao, Y.; Zhao, X.; Hu, Y.; Hao, X.; Xu, L.; Liu, R. A review of a recently emerged technology: Constructed wetland–Microbial fuel cells. *Water Res.* **2015**, *85*, 38–45. [CrossRef]
17. Zhai, X.; Piwpuan, N.; Arias, C.A.; Headley, T.; Brix, H. Can root exudates from emergent wetland plants fuel denitrification in subsurface flow constructed wetland systems? *Ecol. Eng.* **2013**, *61*, 555–563. [CrossRef]
18. Yadav, A.K.; Dash, P.; Mohanty, A.; Abbassi, R.; Mishra, B.K. Performance assessment of innovative constructed wetland-microbial fuel cell for electricity production and dye removal. *Ecol. Eng.* **2012**, *47*, 126–131. [CrossRef]
19. Miri, R.; Chouikhi, A. Ecotoxicological marine impacts from seawater desalination plants. *Desalination* **2005**, *182*, 403–410. [CrossRef]
20. Wang, F.; Xu, C.; Wang, L.; Zhu, P.; Zhang, L.; Wang, X.; Wang, J.; Liu, Q.; Liu, F. Integrated constructed wetland wastewater treatment system comprises wetland wastewater treatment unit, which is used for purification of wetland self-flowing wetland wastewater, and wetland information collection unit, which is used to collect wetland wastewater purification environmental. CN Patent 114590905-A, 07 June 2022.
21. Mu, C.; Wang, L.; Wang, L. Performance of lab-scale microbial fuel cell coupled with unplanted constructed wetland for hexavalent chromium removal and electricity production. *Environ. Sci. Pollut. Res.* **2020**, *27*, 25140–25148. [CrossRef]
22. Fang, Z.; Cheng, S.; Wang, H.; Cao, X.; Li, X. Feasibility study of simultaneous azo dye decolorization and bioelectricity generation by microbial fuel cell-coupled constructed wetland: Substrate effects. *Rsc Adv.* **2017**, *7*, 16542–16552. [CrossRef]

23. Liu, H.; Ramnarayanan, R.; Logan, B.E. Production of electricity during wastewater treatment using a single chamber microbial fuel cell. *Environ. Sci. Technol.* **2006**, *38*, 2281. [CrossRef]
24. Li, D.; Zhao, Y.; Wei, D.; Tang, C.; Wei, T. Key issues to consider toward an efficient constructed wetland-microbial fuel cell: The idea and the reality. *Environ. Sci. Pollut. Res.* **2024**, *31*, 12083–12093. [CrossRef] [PubMed]
25. Kress, N. Actual Impacts of Seawater Desalination on the Marine Environment Reported Since 2001. In *Marine Impacts of Seawater Desalination*; Elsevier: Amsterdam, The Netherlands, 2019.
26. Xiaoying, Z.; Mengqi, J.; Xiang, Z.; Wei, C.; Dan, L.; Yuan, Z.; Xiaoyao, S. Enhanced removal mechanism of iron carbon micro-electrolysis constructed wetland on C, N, and P in salty permitted effluent of wastewater treatment plant. *Sci. Total Environ.* **2018**, *649*, 21–30.
27. Kester, D.R.; Duedall, I.W.; Connors, D.N.; Pytkowicz, R.M. Preparation of Artificial Seawater. *Limnol. Oceanogr.* **1967**, *12*, 176–179. [CrossRef]
28. Liu, J.; Yuan, J.; Ji, Z.; Wang, B.; Hao, Y.; Guo, X. Concentrating brine from seawater desalination process by nanofiltration–electrodialysis integrated membrane technology. *Desalination* **2016**, *390*, 53–61. [CrossRef]
29. Xu, L.; Graham, N.J.D.; Wei, C.; Zhang, L.; Yu, W. Abatement of the membrane biofouling: Performance of an in-situ integrated bioelectrochemical-ultrafiltration system. *Water Res.* **2020**, *179*, 115892. [CrossRef]
30. Xu, D.; Zhang, S.; Tian, W.; Zhang, D.; Chu, M.; Cao, H.; Chen, Z.; Zhang, R. Efficacy and power production performance of constructed wetlands coupled with microbial fuel cells for the advanced treatment of saline tailwater from wastewater treatment plants. *J. Water Process Eng.* **2024**, *60*, 105228. [CrossRef]
31. Ahlawat, O.P.; Yadav, D.; Walia, N.; Kashyap, P.L.; Sharma, P.; Tiwari, R. Root Exudates and Their Significance in Abiotic Stress Amelioration in Plants: A Review. *J. Plant Growth Regul.* **2024**, *43*, 1736–1761. [CrossRef]
32. Oon, Y.-L.; Ong, S.-A.; Ho, L.-N.; Wong, Y.-S.; Dahalan, F.A.; Oon, Y.-S.; Lehl, H.K.; Thung, W.-E.; Nordin, N. Role of macrophyte and effect of supplementary aeration in up-flow constructed wetland-microbial fuel cell for simultaneous wastewater treatment and energy recovery. *Bioresour. Technol.* **2017**, *224*, 265–275. [CrossRef]
33. Wang, R.; Baldy, V.; Perissol, C.; Korboulewsky, N. Influence of plants on microbial activity in a vertical-downflow wetland system treating waste activated sludge with high organic matter concentrations. *J. Environ. Manag.* **2012**, *95*, S158–S164. [CrossRef]
34. Zhu, Y.; Dai, H.; Yuan, S. The competition between heterotrophic denitrification and DNRA pathways in hyporheic zone and its impact on the fate of nitrate. *J. Hydrol.* **2023**, *626*, 130175. [CrossRef]
35. Wang, J.; Song, X.; Wang, Y.; Bai, J.; Bai, H.; Yan, D.; Cao, Y.; Li, Y.; Yu, Z.; Dong, G. Bioelectricity generation, contaminant removal and bacterial community distribution as affected by substrate material size and aquatic macrophyte in constructed wetland-microbial fuel cell. *Bioresour. Technol.* **2017**, *245*, 372–378. [CrossRef] [PubMed]
36. Lefebvre, O.; Tan, Z.; Kharkwal, S.; Ng, H.Y. Effect of increasing anodic NaCl concentration on microbial fuel cell performance. *Bioresour. Technol.* **2012**, *112*, 336–340. [CrossRef] [PubMed]
37. Xu, F.; Ouyang, D.-L.; Rene, E.R.; Ng, H.Y.; Guo, L.-L.; Zhu, Y.-J.; Zhou, L.-L.; Yuan, Q.; Miao, M.-S.; Wang, Q.; et al. Electricity production enhancement in a constructed wetland-microbial fuel cell system for treating saline wastewater. *Bioresour. Technol.* **2019**, *288*, 121462. [CrossRef] [PubMed]
38. Xin, X.; Xie, J.; Li, W.; Lv, S.; He, J. New insights into microbial fuel cells for saline wastewater treatment: Bioelectrogenesis evaluation, microbial interactions and salinity resource reuse. *Process Saf. Environ. Prot.* **2022**, *168*, 314–323. [CrossRef]
39. Parida, A.K.; Das, A.B.; Mittra, B. Effects of salt on growth, ion accumulation, photosynthesis and leaf anatomy of the mangrove. *Trees-Struct. Funct.* **2004**, *18*, 167–174. [CrossRef]
40. Kumar, S.S.; Kumar, V.; Gude, V.G.; Malyan, S.K.; Pugazhendhi, A. Alkalinity and salinity favor bioelectricity generation potential of *Clostridium*, *Tetrathiobacter* and *Desulfovibrio* consortium in Microbial Fuel Cells (MFC) treating sulfate-laden wastewater. *Bioresour. Technol.* **2020**, *306*, 123110. [CrossRef]
41. Guo, F.; Luo, H.; Shi, Z.; Wu, Y.; Liu, H. Substrate salinity: A critical factor regulating the performance of microbial fuel cells, a review. *Sci. Total Environ.* **2021**, *763*, 143021. [CrossRef]
42. Gao, F.; Liu, G.; She, Z.; Ji, J.; Gao, M.; Zhao, Y.; Guo, L.; Jin, C. Effects of salinity on pollutant removal and bacterial community in a partially saturated vertical flow constructed wetland. *Bioresour. Technol.* **2021**, *329*, 124890. [CrossRef]
43. Wang, X.; Zhu, H.; Yan, B.; Shutes, B.; Banuelos, G.; Wen, H. Bioaugmented constructed wetlands for denitrification of saline wastewater: A boost for both microorganisms and plants. *Environ. Int.* **2020**, *138*, 105628. [CrossRef]
44. Liang, Y.; Zhu, H.; Banuelos, G.; Yan, B.; Shutes, B.; Cheng, X.; Chen, X. Removal of nutrients in saline wastewater using constructed wetlands: Plant species, influent loads and salinity levels as influencing factors. *Chemosphere* **2017**, *187*, 52–61. [CrossRef]
45. Hadad, H.R.; Maine, M.A.; Bonetto, C.A. Macrophyte growth in a pilot-scale constructed wetland for industrial wastewater treatment. *Chemosphere* **2006**, *63*, 1744–1753. [CrossRef] [PubMed]
46. Wu, Y.; Tam, N.F.Y.; Wong, M.H. Effects of salinity on treatment of municipal wastewater by constructed mangrove wetland microcosms. *Mar. Pollut. Bull.* **2008**, *57*, 727–734. [CrossRef] [PubMed]

47. Srivastava, P.; Yadav, A.K.; Mishra, B.K. The effects of microbial fuel cell integration into constructed wetland on the performance of constructed wetland. *Bioresour. Technol.* **2015**, *195*, 223–230. [CrossRef] [PubMed]
48. Das, B.; Thakur, S.; Chaithanya, M.S.; Biswas, P. Batch investigation of constructed wetland microbial fuel cell with reverse osmosis (RO) concentrate and wastewater mix as substrate. *Biomass Bioenergy* **2019**, *122*, 231–237. [CrossRef]
49. Kong, Q.; He, X.; Feng, Y.; Miao, M.-s.; Wang, Q.; Du, Y.-d.; Xu, F. Pollutant removal and microorganism evolution of activated sludge under ofloxacin selection pressure. *Bioresour. Technol.* **2017**, *241*, 849–856. [CrossRef]
50. Jung, S.; Regan, J.M. Comparison of anode bacterial communities and performance in microbial fuel cells with different electron donors. *Appl. Microbiol. Biotechnol.* **2007**, *77*, 393–402. [CrossRef]
51. Zhao, N.; Jiang, Y.; Alvarado-Morales, M.; Treu, L.; Angelidaki, I.; Zhang, Y. Electricity generation and microbial communities in microbial fuel cell powered by macroalgal biomass. *Bioelectrochemistry* **2018**, *123*, 145–149. [CrossRef]
52. Chu, N.; Zhang, L.; Hao, W.; Liang, Q.; Jiang, Y.; Zeng, R.J. Rechargeable microbial fuel cell based on bidirectional extracellular electron transfer. *Bioresour. Technol.* **2021**, *329*, 124887. [CrossRef]
53. Kong, Y.; Tao, M.; Lu, X.; Cheng, C.; Jing, Z. Study on the performance of accessory microbial fuel cell (MFC) integrated to the constructed wetlands (CWs) for deep wastewater treatment. *Desalination Water Treat.* **2024**, *318*, 100358. [CrossRef]
54. Wang, L.; Pang, Q.; Zhou, Y.; Peng, F.; He, F.; Li, W.; Xu, B.; Cui, Y.; Zhu, X. Robust nitrate removal and bioenergy generation with elucidating functional microorganisms under carbon constraint in a novel multianode tidal constructed wetland coupled with microbial fuel cell. *Bioresour. Technol.* **2020**, *314*, 123744. [CrossRef]
55. Doherty, L.; Zhao, Y.; Zhao, X.; Wang, W. Nutrient and organics removal from swine slurry with simultaneous electricity generation in an alum sludge-based constructed wetland Incorporating microbial fuel cell technology. *Chem. Eng. J.* **2015**, *266*, 74–81. [CrossRef]
56. Liu, S.; Feng, X.; Xue, H.; Qiu, D.; Huang, Z.; Wang, N. Bioenergy generation and nitrogen removal in a novel ecological-microbial fuel cell. *Chemosphere* **2021**, *278*, 130450. [CrossRef]